AAS 11-534

PRELIMINARY ANALYSIS FOR THE NAVIGATION OF MULTIPLE-SATELLITE-AIDED CAPTURE SEQUENCES AT JUPITER

Alfred E. Lynam*, James M. Longuski†

Multiple-satellite-aided capture employing gravity assists of more than one Galilean moon can help capture a spacecraft into orbit about Jupiter. Each additional moon flyby reduces the propulsive ΔV required for Jupiter capture. While the existence of these trajectories has been demonstrated deterministically, the challenges associated with actually navigating a spacecraft through several close flybys in rapid succession are nontrivial. This paper addresses these navigation challenges by using simulated observations to estimate a spacecraft's orbit as it approaches Jupiter and by targeting trajectory correction maneuvers to guide the spacecraft through multiple-satellite-aided capture sequences. Results indicate that radiometric navigation alone can easily provide safe double-satellite-aided capture sequences using a ballistic strategy, i.e. without any trajectory correction maneuvers (TCMs) in between flybys. However, triple-satellite-aided capture sequences require the operational capacity to target TCMs in between flybys in order to be feasible.

INTRODUCTION

The use of gravity-assist flybys of moons to reduce the ΔV required to capture a spacecraft into orbit around a planet is called satellite-aided capture. Satellite-aided capture was first proposed for Jupiter missions by Longman[1] and Longman and Schneider.[2] They calculated the Galilean moons' capacity to decrease in the orbital energy of a spacecraft via gravity assist for sequences involving flybys of one or two moons.

Cline,[3] Nock and Uphoff,[4] MacDonald and McInnes,[5] Yam,[6] and Okutsu et al.[7] have all made substantial contributions to the single-satellite-aided capture problem. A single-satellite-aided capture sequence with an Io gravity-assist was used to capture Galileo into orbit around Jupiter, saving 175 m/s of ΔV.[8] Some initial mission design of double-satellite-aided capture sequences has been done by Nock and Uphoff,[4] Johannesen and D'Amario,[9] Landau et al.[10]

Lynam et al.[11] discovered triple- and quadruple-satellite-aided capture sequences at Jupiter and extended the mission design of double-satellite-aided capture sequences. They estimated the ΔV savings and sensitivity to flyby altitude errors of each type of multiple-satellite-aided capture sequence using a patched-conic model and integrated high-fidelity trajectories in AGI's STK.[12] Lynam and Longuski[13] extended this analysis by finding interplanetary trajectories from Earth to Jupiter that used double- or triple-satellite-aided capture to achieve orbit about Jupiter.

*Doctoral Student, School of Aeronautics & Astronautics, Purdue University, 701 W. Stadium Ave. West Lafayette, IN 47907-2045. Student Member AIAA.

†Professor, School of Aeronautics & Astronautics, Purdue University, 701 W. Stadium Ave. West Lafayette, IN 47907-2045. Associate Fellow AIAA and Member AAS.

There has been no published work on the navigation of multiple-satellite-aided capture sequences, however, the actual navigation of Galileo's single-satellite-aided capture sequence that used an Io gravity assist has been documented by Haw et al.[14] Due to a tape recorder anomaly in the Galileo spacecraft, no optical images were available for navigation, so Galileo's single-satellite-aided capture sequences was exclusively navigated using radiometric tracking data. Due to the lack of optical navigation, the orbit determination errors of the Io gravity assist were rather large (1σ altitude errors of about 30 km and out-of-plane errors of 70 km).[14]

While planning for the delayed Europa orbiter mission, Guman et al.[15] performed a navigation feasibility study for a sample mission with an Io single-satellite-aided capture sequence and Raofi et al.[16] performed a statistical ΔV analysis for a different sample mission with a Ganymede single-satellite-aided capture sequence. In the navigation feasibility study with the Io flyby, the 1σ altitude errors were also about 30 km, but the out-of-plane errors were close to 40 km.[15]

Although 30-km altitude errors are acceptable for single-satellite-aided capture sequences, much higher precision is needed for multiple-satellite-aided capture. Lynam et al.[11] showed that flyby errors will geometrically propagate to subsequent flybys. For example, in a Ganymede-Io double-satellite-aided capture sequence, a 40-km altitude error in the Ganymede flyby will ballistically propagate to a 340-km altitude error in the Io flyby.

This paper applies the navigation techniques discussed above to solve the navigation problem for multiple-satellite-aided capture. In our model, we simulate a set of observations from a spacecraft approaching Jupiter, determine its covariance using navigation filtering techniques, and estimate the required statistical ΔV by targeting trajectory correction maneuvers. The trajectory correction manuevers are tested within a Monte Carlo simulation to determine the ΔV statistics for a variety of maneuver times and targeting strategies.

NOMINAL TRAJECTORY DESIGN

Patched-conic Results

Lynam et al.[11] estimated the deterministic ΔV required to capture a spacecraft into orbit around Jupiter via multiple-satellite-aided capture by using a patched-conic method. Within this circular, coplanar, patched-conic method, the gravity assists of Jupiter's moons are modeled as instantaneous decreases in the spacecraft's Jovicentric orbital energy and perijove. The spacecraft's trajectory is propagated between gravity assists using Jupiter-centered conic sections. A Jupiter orbit insertion (JOI) maneuver is added at perijove to complete the capture sequences. These patched-conic ΔV estimates for varying numbers of gravity assists of the Jovian moons and various perijove radii are tabulated in Table 1. A more detailed description of this patched-conic method and more complete results for the deterministic ΔV's for multiple-satellite-aided capture sequences are available in Lynam et al.[11]

These deterministic ΔV estimates will guide our choices of sequences to investigate further. The double-satellite-aided capture sequences that require the least deterministic ΔV are Ganymede and Io sequences, and the triple-satellite-aided capture sequences that require the least deterministic ΔV are Callisto, Ganymede, and Io sequences. We will also focus on sequences that finish their gravity assists before their JOI maneuvers, because the JOI maneuver will introduce additional error in subsequent flybys. Thus, the two sequences that we will investigate in more detail are Ganymede-Io-JOI sequences and Callisto-Ganymede-Io-JOI sequences. Ganymede-Io-JOI sequences would perform

Table 1. ΔV for Best Jupiter Capture[a], m/s

Flyby Sequences	JOI (5 R_J)[b] ΔV, m/s	JOI (4 R_J) ΔV, m/s	JOI (3 R_J) ΔV, m/s	JOI (2 R_J) ΔV, m/s	JOI (1.01 R_J) ΔV, m/s
Unaided	825	735	641	524	371
Best Single	556	526	483	416	308
Best Double	330	340	333	299	228
Best Triple	202	232	245	234	190
Best Quadruple	—	—	—	175	160

[a] Arrival C_3 is 31.36 km^2/s^2, flyby altitudes are fixed at 300 km, and the spacecraft captures into a 200-day orbit.
[b] R_J=71,492 km.

close flybys of Ganymede and Io before executing a JOI maneuver, while Callisto-Ganymede-Io-JOI sequences would also include a Callisto flyby before the other two flybys.

Integrated Interplanetary Trajectories

Lynam and Longuski[13] used AGI's STK[12] to find high-fidelity interplanetary trajectories from Earth to Jupiter capture that included multiple-satellite-aided capture sequences. The STK propagator model includes the best available gravity fields of Jupiter and its moons, the Sun's point-mass gravity, solar radiation pressure, and general relativity perturbations. The interplanetary trajectories that used double-satellite-aided capture sequences (e.g. Ganymede-Io-JOI sequences) did not require any deterministic deep space maneuvers between Earth and Jupiter, but the trajectories that included triple-satellite-aided capture sequences required between 40 m/s (for a particular Ganymede-Io-JOI-Europa sequence) and 100 m/s (for a particular Callisto-Ganymede-Io-JOI sequence) of deterministic ΔV to target the sequences. For these two particular trajectories, the deep space maneuver (DSM) ΔV required to target the triple-satellite-aided capture sequences offsets the potential JOI ΔV savings of using triple-satellite-aided capture vs double-satellite-aided capture. However, an exhaustive search of all triple-satellite-aided capture sequences has yet to be completed, so it is possible that some triple-satellite-aided capture sequences may require less deterministic ΔV than double-satellite-aided capture sequences.

We are focusing on Ganymede-Io-JOI sequences and Callisto-Ganymede-Io-JOI sequences for our navigation analysis to avoid the complexity of including a JOI maneuver in between flybys, so we select two nominal interplanetary trajectories that include these capture sequences. We only use direct Earth-Jupiter trajectories for simplicity, but Lynam and Longuski[13] showed that these direct trajectories could be extended to form interplanetary trajectories that include additional gravity assists of Venus, Earth, or Mars. The Callisto-Ganymede-Io-JOI sequence is suboptimal because it has a much higher arrival C_3 (47.7 km^2/s^2) than a Hohmann transfer (31.4 km^2/s^2) and a 100 m/s DSM, but its statistical ΔV requirements should be roughly equivalent to a better Callisto-Ganymede-Io-JOI trajectory. For the statistical ΔV analysis, the most important properties of the trajectories are their encounter times, flyby altitudes, and B-plane angles, so these are included in Tables 2 and 3. (A derivation of B-plane parameters is included in the appendix.)

Table 2. Integrated GIJ Flyby Sequence: Flyby Parameters

Encounter Times, UTC	Encounter	B-plane angle, deg	h_p, km
16 June 2022 5:17	Earth	—	—
29 Aug 2024 19:22	Ganymede	0.0	300.8
30 Aug 2024 5:53	Io	45.4	356.9
30 Aug 2024 10:10	Jupiter	—	—

Table 3. Integrated CGIJ Flyby Sequence: Flyby Parameters

Encounter Times, UTC	Encounter	B-plane angle, deg	h_p, km
27 Feb 2021 23:39	Earth	—	—
14 Dec 2023 14:19	Callisto	0.0	250.4
15 Dec 2024 7:00	Ganymede	-21.1	446.0
15 Dec 2024 17:50	Io	-0.1	376.2
15 Dec 2025 22:16	Jupiter	—	—

LOW-ORDER COVARIANCE ANALYSIS

Observations

The first step of our navigation analysis is a statistical orbit determination covariance analysis. We employ three different orbit determination strategies: a purely radiometric strategy, a combined radiometric and optical navigation strategy, and a purely optical navigation strategy (to simulate autonomous optical navigation.) Radiometric observables include the range, the range-rate (a simplification of Doppler data), and the right ascension and declination angles (a simplification of Δ-DOR or Δ-VLBI) of the spacecraft as observed from the DSN tracking stations on Earth. Optical observables are the right ascension and declination angles (a simplification of the picture taking and image processing involved in OpNav) of the Galilean moons as observed from the spacecraft.

In our simplified model, we assume that each simulated observation has an error that is distributed around its actual value via a gaussian distribution. The standard deviations of these distributions are recorded in Table 4. The standard deviations for the radiometric observables are loosely based on the standard deviations or data residuals from the Mars Exploration Rover (MER)[17] and Cassini missions.[18] The optical navigation errors are based on the notional narrow angle camera for the 2008 JEO mission study.[19] This camera has a 1.17 degree field of view and can produce OpNav images that are stored as 2048 by 2048 arrays of digital pixels. We assume that attitude knowledge, star-tracking, limb-scanning, and center-finding techniques can determine the angular direction from the spacecraft to the centers of the Galilean moons to within 0.1 pixels, which corresponds to about 1 μrad in right ascension and declination. This 0.1 pixel standard deviation is similar to those used in the Cassini approach phase to Saturn.

Table 4. Standard Deviations of Simulated Observations

Observable	Simulated 1-σ Error
Range from Earth	5 m
Range-rate from Earth	0.5 mm/s
Radiometric RA and Dec angles from Earth	5 nrad
OpNav RA and Dec angles to moons	1 μrad

Estimated States

State estimation is the next stage of our low-order covariance analysis. We use an Earth-centered J2000 coordinate system in our state (position and velocity) estimates when we use navigation techniques that include radiometric observations. In those cases, the ephemerides of the Galilean moons and Jupiter are used as additional states in order to estimate the state of the spacecraft with respect to these bodies. This methodology allows the Earth-centered state of the spacecraft and the Earth-centered positions of the Galilean moons and Jupiter to be updated simultaneously within the orbit determination filter. For OpNav-only navigation techniques, we only track the relative state of the spacecraft with respect to each of the Galilean moons, since no Earth-relative information is assumed to be available.

We use the same STK state propagation model for our low-order covariance analysis as we used for the nominal trajectory. The state transition matrix between the spacecraft's state at the time of an observation and its state at an orbit determination epoch is calculated numerically by integrating six trajectories that are slightly perturbed from the nominal trajectory (each perturbed in one of the six position and velocity states) and using finite differencing. The state transition matrix between the states and the ephemerides is integrated using a separate numerical integrator within MATLAB. This numerical integrator only uses the point-mass gravity of the Sun, Jupiter, and the Galilean moons to propagate this portion of the state transition matrix, so it is less accurate than the STK integrator. However, use of a less precise propagator is consistent with the low-order nature of this covariance analysis, so it is good enough for our preliminary navigation analysis.

The simulated observations are used to estimate the covariance spacecraft's state and ephemerides via a batch sequential filter. The filter was constructed using a combination of batch and Kalman filtering techniques. The observations are processed in one day "batches" by using state transition matrices to map all the simulated observations during a single day to the beginning of that day. The resulting covariance matrix at the beginning of that day is stored and propagated (via the state transition matrix) to the end of that day. The resulting covariance matrix at the end of the first day of observations is used as an initial covariance matrix for the processing of the second day of observations (demonstrating the sequential aspect of the filter). This process is repeated in one day increments until the spacecraft is a few days away from its first flyby of one of the Galilean moons.

Radiometric-Only Tracking

The first orbit determination tracking technique we used was radiometric navigation with no OpNav pictures. Thus, only the first 3 observables (range, range-rate, and angular data with respect

to Earth) in Table 4 were used in this covariance analysis. The radiometric observations were simulated using the ephemerides of the positions of the largest Deep Space Network (DSN) Earth-based radiometric tracking stations (at Goldstone, CA, Canberra, Australia, and Madrid, Spain). In this low-order covariance analysis, we simulated the range and range-rate observables by finding the actual range and range rate of the spacecraft from each tracking station and perturbing it by Gaussian random variables with mean zero and standard deviations equivalent to those in Table4. Range and range-rate data were only recorded from one station at a time (the station facing the spacecraft at that time). Angular data are only collected when two stations are facing the spacecraft at the same time.

This navigation strategy is similar to the strategy used by the Galileo spacecraft as it approached Jupiter because of Galileo's lack of OpNav capacity.[14] The key difference between Galileo's use of only radiometric data and the use of only radiometric data for a future mission is that the ephemerides of the Galilean moons are now better known because of the data collected by Galileo during its satellite tour of the Galilean moons. While the ephemerides of the Galilean moons that were used by Galileo had errors of more than 100 kilometers,[20] the current ephemerides have estimated errors of only 5 kilometers in each direction.[21] Additionally, Jupiter's position with respect to Earth is much better known than it was during the Galileo mission and will be known even more precisely after the Juno mission.[22] The estimated *a priori* ephemeris knowledge error of Jupiter's position with respect to Earth is assumed to be 15 kilometers in each direction.

The low-order covariance analysis for radiometric-only navigation begins about one month before the spacecraft reaches the Galilean moons. The radiometric observations can quickly and precisely determine the spacecraft's state with respect to Earth, but determining the spacecraft's state with respect to Jupiter requires more observations and cannot be known as precisely. The spacecraft's state with respect to a Galilean moon cannot be determined radiometrically until the spacecraft performs a flyby of that moon, so the radiometric-only navigation technique relies strongly on the accuracy of the *a priori* ephemerides of the Galilean moons to target the flybys of the moons.

Autonomous Optical Navigation

The second orbit determination technique we analyze is using only optical navigation. In this analysis, we assume that the spacecraft is operating autonomously from Earth, so it would only have access to its own OpNav pictures to navigate itself. Although the process of extracting useful orbit determination observables from OpNav images is complex in practice,[23] we assume that the spacecraft can autonomously process the OpNav images to provide angular information about the spacecraft's position relative to the Galilean moons. For simplicity, all four Galilean moons are modeled to be tracked simultaneously. Hence, each observation contains 8 observables: right ascension (RA) and declination (Dec) angles for each moon. Realistically, it is unlikely that all four moons would be in a single OpNav image's frame at the same time, so we assume that multiple OpNav images are taken per observation. In our simplified OpNav model, we further assume that the OpNav images are uninterrupted and taken at a constant rate. Thus, we do not consider eclipses of the Galilean moons with each other or with Jupiter. We also do consider interruptions due to other operational requirements for the spacecraft. Because of these assumptions, the actual rate of pictures would have to be faster than our modeled rate to get the same results.

Autonomous Optical navigation has been used by two missions: Deep Space 1[24,25] and Deep Impact.[26,27] Deep Space 1 was a technology demonstrator mission that performed autonomous flybys of the asteroid Braille and the comet Borrelly. Deep Impact was composed of two spacecraft:

a spacecraft that performed a flyby of comet Tempel 1 and a spacecraft that impacted comet Tempel 1. Normal radiometric and optical navigation were performed until the impactor was 2 hours away from its collision with comet Tempel 1. The final two hours of the impact trajectory were navigated by the spacecraft completely autonomously. Three maneuvers were executed in the minutes before impact, so the impact was able to be controlled to within 250 meters of its aimpoint.[27]

Because of the dynamical sensitivity of multiple-satellite-aided capture sequences, the extremely precise targeting of Deep Impact's AutoNav would be useful in navigating these sequences. However, there are several important differences between the navigation problems of targeting a comet impact and targeting several successive close flybys of the massive Galilean moons. First of all, the *a priori* ephemerides of the Galilean moons are far more accurate than those of a comet or asteroid. The surfaces and rotation rates of the Galilean moons are much better defined than those of comets. The Galilean moons are also several orders of magnitude larger than comets, so using OpNav to perform centerfinding would be more difficult as the spacecraft approaches a moon and its OpNav frame becomes completely encompassed by the moon. In this scenario, traditional OpNav would not be effective when the spacecraft gets too close to a moon, so landmark optical navigation, radar navigation, or lidar navigation may become necessary to autonomously navigate the spacecraft as it approaches a moon.[28−30] These advanced flyby navigation concepts are beyond the scope of this preliminary analysis, however, so we end our AutoNav analysis a few days before the first flyby of a multiple satellite-aided capture sequence.

The results of the low-order covariance analysis for autonomous optical navigation indicate that the position of the spacecraft relative to the Galilean moons can be determined to within a few kilometers about 3 days before a multiple-satellite-aided capture sequence begins. In particular, the position of the spacecraft relative to Ganymede, Europa, and Callisto can be determined with an accuracy of approximately 1 kilometer if we assume OpNav observations of all four Galilean moons every 5 minutes for 25 days. The spacecraft's relative position to Io has an error of more than 2 kilometers because its orbit is closer to Jupiter than the other Galilean moons. If we assume OpNav observations of all four Galilean moons every hour for 25 days, the position errors are about 8 kilometers for Io, 4 kilometers for Europa, and 3 kilometers for Callisto and Ganymede. The first flybys of our nominal trajectories in Tables 2 and 3 are Ganymede and Callisto, respectively, so the better knowledge of the spacecraft-relative positions of these moons would decrease the error in the first flyby of each sequence. Because flyby errors propagate geometrically in these multiple-satellite-aided capture sequences,[11] decreasing the error in the first flyby of these sequences can greatly decrease the error in subsequent flybys if there are no trajectory correction maneuvers in between flybys.

Combined Radiometric and Optical Navigation

The final orbit determination strategy involves both radiometric and optical navigation. Unlike both the radiometric-only strategy and the autonomous optical navigation strategy, this strategy can actually provide knowledge of the spacecraft's position with respect to Earth with radiometric data and update the ephemeris positions of Jupiter and its Galilean moons with OpNav data. In our low-order covariance model, the position and velocity of a spacecraft with respect to Earth using this stategy is known precisely, so the covariance update of the ephemerides of Jupiter and its Galilean moons is the primary result of this analysis. Figure 1 shows the improvement of the ephemerides of Jupiter and the Galilean moons over 26 days of observation.

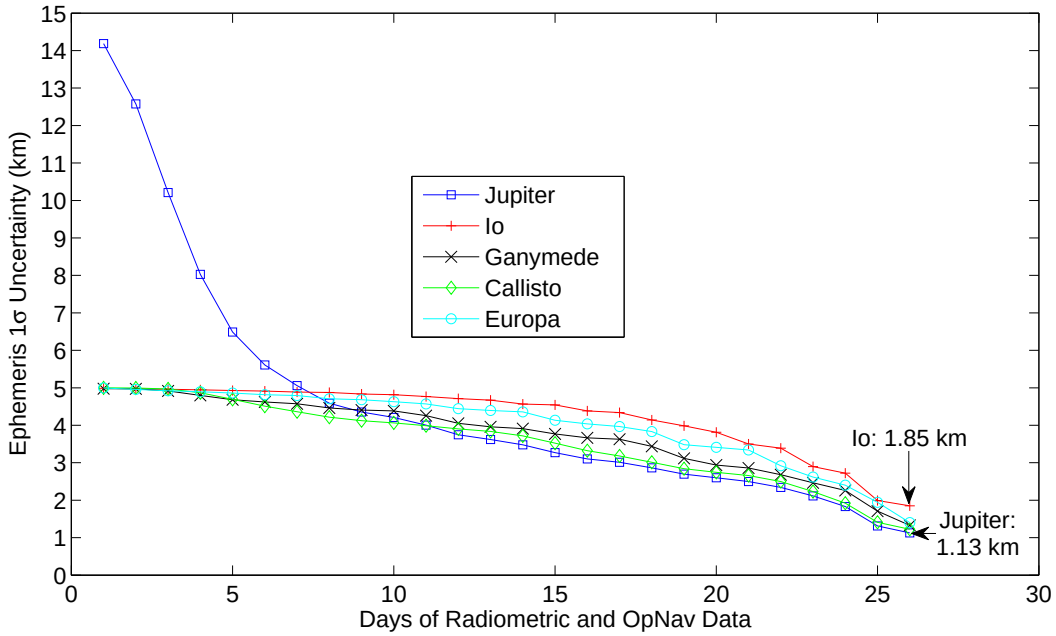

Figure 1. Covariance results for combined radiometric and optical navigation for Jupiter approach. The picture rate is one OpNav image of each moon every 5 minutes. We note that the data collection ends 2–3 days before the first flyby of the multiple-satellite-aided capture sequence.

ESTIMATING THE STATISTICAL ΔV: MONTE CARLO SIMULATIONS

After the covariance analysis, we estimate the statistical ΔV of the two multiple-satellite-aided capture sequences described in Tables 2 and 3 using various navigation strategies. For some of these strategies, we limit the number of trajectory correction maneuvers (TCMs) and allow the flyby sequences to be mostly ballistic. In these cases the trajectory will be less controlled, so the flyby altitude errors will be allowed to become larger. The remainder of these navigation strategies will include several TCMs, including TCMs in between flybys. Each of these navigation strategies is tested via Monte Carlo simulation by applying gaussian perturbations to the nominal values of the input random variables.

Statistical Maneuver Execution Error Model

In our statistical ΔV analysis, we model the statistics of the TCMs with an early maneuver execution error model used for Cassini's interplanetary trajectory by Goodson et al.[31] We use this model rather than the more refined models used later in the mission by Wagner and Goodson[32] and Gist et al.[33] because the spacecraft approaching Jupiter will likely have maneuver execution errors more similar to the maneuver execution errors of the early Cassini mission rather than the maneuver execution errors modeled after the end of Cassini's prime mission. As in Raofi et al.,[16] Goodson et al.,[31] and Gist et al.,[33] we use a spherical maneuver execution error model that was developed by Gates.[34] Gates's maneuver execution model includes fixed and proportional errors for the magnitude of each TCM and fixed and proportional errors for the angular components of each TCM (i.e. pointing errors). These fixed and proportional magnitude and pointing errors are exactly

Table 5. TCM: Maneuver Execution Error Model[31]

Error Type	1-σ Error
Fixed Magnitude	3.5 mm/s
Proportional Magnitude	2.0 %
Fixed Pointing	3.5 mm/s
Proportional Pointing	8.5 mrad

the same as Cassini's RCS thruster error model used by Goodson et al. and are listed in Table 5.

The maneuver execution error model is incorporated into each Monte Carlo simulation after each nominal TCM is calculated. Each nominal TCM ΔV vector is perturbed in its magnitude direction and two pointing directions by adding gaussian, mean zero random variables with standard deviations calculated from the nominal TCM ΔV and the errors in Table 5. If a navigation strategy uses multiple TCMs, each nominal TCM is calculated and perturbed independently.

Monte Carlo Simulation Setup

We use the high-fidelity STK propagator described earlier in the paper to propagate the Monte Carlo simulations. The Monte Carlo simulation begins a few days before the spacecraft's first flyby. The spacecraft's nominal position is perturbed in all 3 directions by gaussian random errors with standard deviations of 15 kilometers to simulate the *a priori* error in the spacecraft's position with respect to Jupiter. The spacecraft is then propagated until one day before its first flyby, which is the maneuver epoch of TCM 1. The desired B-plane parameters of the first flyby of the sequence are perturbed by a random error corresponding to the knowledge error of the spacecraft's position with respect to the first moon. (This knowledge error depends on whether a particular navigation strategy uses OpNav or not.) These perturbed B-plane parameters are targeted using the three vector coordinates of the ΔV vector. This nominal ΔV vector is then perturbed using the maneuver execution error model to give the perturbed TCM 1 ΔV vector.

After the perturbed TCM 1 ΔV vector is applied to the trajectory one day before the first flyby, the trajectory is propagated through the remainder of the sequence for ballistic navigation strategies or until the desired time of TCM 2 for navigation strategies that include TCMs in between flybys. For ballistic strategies, the B-plane errors of the subsequent flybys are the main results of the Monte Carlo simulations. If these B-plane errors are too large, the spacecraft may have a substantial risk of colliding with one of the Galilean moons. If the ballistic B-plane errors are acceptable for a particular multiple-satellite-aided capture sequence, then this particular capture sequence would be feasible with present navigation mechods and not depend on developing the operational ability to plan and execute TCMs in between flybys.

The navigation strategies that involve TCMs in between flybys are characterized by the amount of statistical ΔV required to execute these sequences and their operational difficulty. Navigation strategies that include TCMs soon after a flyby would be more operationally difficult than strategies that allowed more time for orbit determination and manevuer planning before the TCMs. However, this extra operational time is offset by inceased statistical ΔV requirements if the trajectory is

corrected later. Since it is difficult to quantify operational complexity in this context, we simply provide a TCM's maneuver time (in hours after flyby) as an informal operational complexity metric. TCM 2 (or TCM 3 for triple-satellite-aided capture sequences) is computed and perturbed using the same methodology as TCM 1. The process is repeated until the simulated spacecraft completes its multiple-satellite-aided capture sequence. The spacecraft's statistical ΔV usage, its maneuver times, and its B-plane errors are recorded in a text file and the process is repeated 100 times to extract useful ΔV and B-plane statistics for each sequence and strategy. Figure 2 summarizes the order of events for these Monte Carlo simulations.

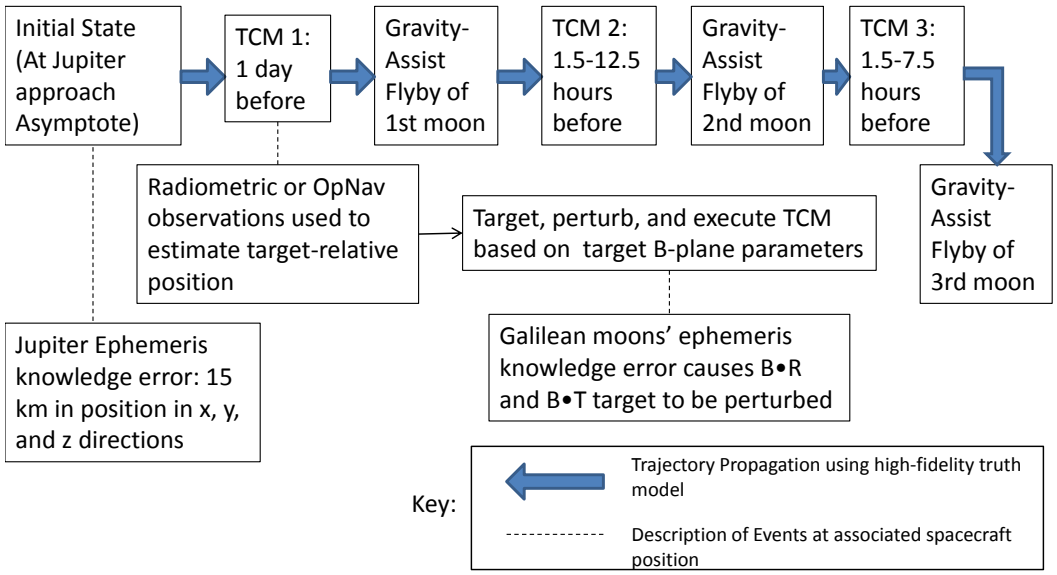

Figure 2. Flowchart for Monte Carlo simulations to estimate statistical ΔV of triple-satellite-aided capture sequences. TCM 1 is in every simulation, but TCMs 2 and 3 are only used with certain navigation strategies.

MONTE CARLO RESULTS

Ballistic Navigation Strategies

Although the strategies we call "ballistic" do include TCM 1 before any of the flybys, the flyby sequence itself is a ballistic flyby sequence because no TCMs occur during the sequence. Because flyby errors propagate geometrically throughout each flyby sequence, the ballistic strategy relies on minimizing the flyby error of the first flyby in a sequence to mitigate the errors in the subsequent flyby(s). Two different orbital determination techniques are used for ballistic navigation strategies, radiometric-only and OpNav-only. For both of these techniques, the spacecraft's trajectory is determined as precisely as possible a few days before the spacecraft's first flyby. The covariances of these trajectories are used to generate the B-plane errors that are used for targeting the first flyby

with TCM 1 within the Monte Carlo simulation.

For radiometric navigation, the *a priori* position errors of the Galilean moons (5 km in each direction) and the estimated position of the spacecraft with respect to Jupiter (using the radiometric data) are incorporated into the B-plane error in the first flyby. (A derivation of B-plane parameters is included in the appendix.) Because radiometric navigation allows more precise in-plane position knowledge than out of plane position knowledge, the $\mathbf{B} \cdot \mathbf{T}$ error of the first flyby is 5 km and the $\mathbf{B} \cdot \mathbf{R}$ error of the first flyby is 7 km. By adding optical navigation, the B-plane error of the first flyby can be reduced to 2 km in the $\mathbf{B} \cdot \mathbf{T}$ direction and 3 km in the $\mathbf{B} \cdot \mathbf{R}$ direction. For both cases, once TCM 1 is targeted (using the perturbed B-plane data) and perturbed using the maneuver execution error model, the remainder of the trajectory is propagated and the B-plane errors are recorded.

For the nominal Callisto-Ganymede-Io-JOI triple-satellite-aided capture sequence described by Table 3, the Monte Carlo simulation B-plane results are plotted in figure 3. Due to the geometric propagation of errors for these ballistic sequences, 21 of the 100 Monte Carlo simulations for the radiometric navigation case would result in the spacecraft crashing into Io. If optical navigation is added, only 1 out of the 100 cases crashes into Io. Thus, ballistic triple-satellite-aided capture strategies are clearly not feasible if only radiometric navigation is used. Even if optical navigation is also used, there is still a substantial collision risk for our nominal trajectory. The collision risk could be lowered if the Io flyby had a higher nominal altitude, but that strategy would still require a substantial amount of statistical ΔV to fix the B-plane errors, reducing the ΔV savings from using triple-satellite-aided capture. For the above reasons, ballistic strategies for triple-satellite-aided capture are not recommended.

Ballistic navigation is much more effective for double-satellite-aided capture sequences because they are less sensitive to initial conditions. For our nominal Ganymede-Io-JOI sequence, both the radiometric-only ballistic navigation strategy and the combined radiometric and optical navigation strategy were effective enough to prevent spacecraft collisions with Io. Figure 4 shows the Io B-plane errors for the 100 Monte Carlo simulations for both navigation strategies. These results show that ballistic strategies are feasible for double-satellite-aided capture sequences (within the assumptions of our models). Since current radiometric and optical navigation techniques are thus sufficient to navigate double-satellite-aided capture, the development of advanced navigation technologies or operational capabilities is not necessary (although it would be beneficial) for navigating double-satellite-aided capture sequences.

Navigation Strategies with Multiple TCMs

Since ballistic navigation strategies are risky for triple-satellite-aided capture and feasible but not optimal for double-satellite-aided capture, we investigate navigational strategies that involve trajectory correction maneuvers in between flybys. For our nominal trajectories, the spacecraft would travel for about 17 hours between its flybys of Callisto and Ganymede, and about 10.5 hours between its flybys of Ganymede and Io. Cassini's double flybys had transfer durations of between 1.5 and 2 days (36 and 48 hours) in between flybys,[35] but TCMs were not used after the first flyby to target the final flyby because the Cassini mission only used TCMs that occurred at least 2 or 3 days after a flyby. In order to implement TCMs in between flybys for multiple-satellite-aided capture sequences, we assume an autonomous flyby navigation or a ground-based flyby navigation that is much faster than Cassini's navigation.

Since the TCMs allow for precise targeting of each flyby (usually within 10 kilometers), the

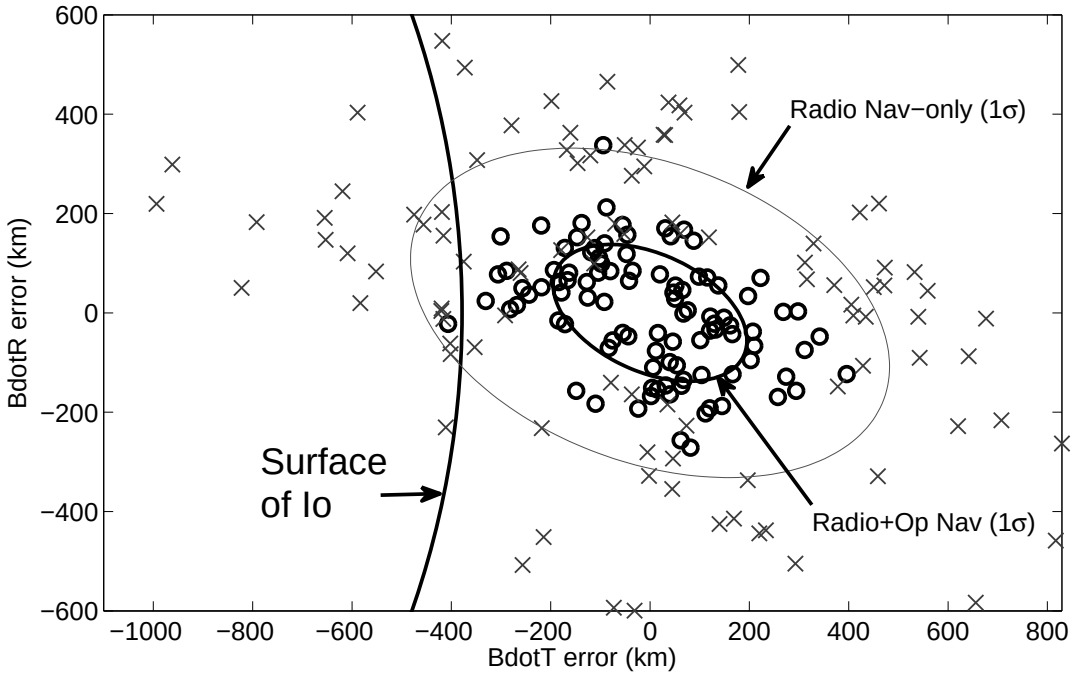

Figure 3. Io B-plane results for ballistic navigation strategies for CGIJ triple-satellite-aided capture sequences. The bold circles represent the B-plane results for combined optical and radiometric navigation. The X's represent the B-plane results for only radiometric navigation. Even with combined radiometric and optical navigation, these results indicate an unacceptable level of risk (1 crash in 100 flybys).

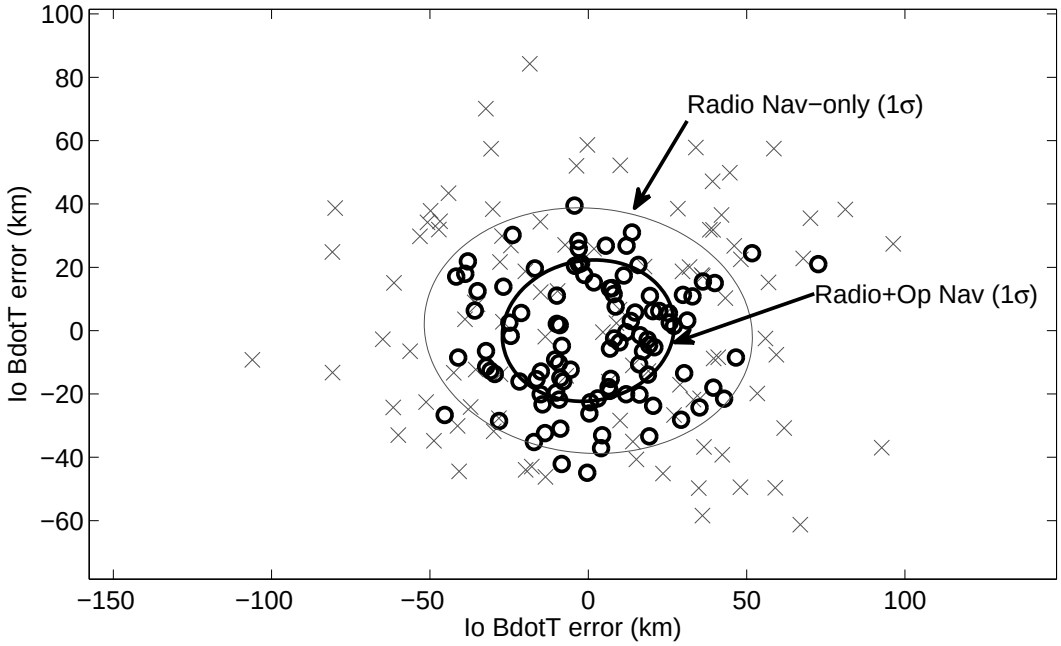

Figure 4. Io B-plane results for ballistic navigation strategies for GIJ double-satellite-aided capture sequences. The bold circles represent the B-plane results for combined optical and radiometric navigation. The X's represent the B-plane results for only radiometric navigation. In either strategy, these results indicate an acceptable level of risk since the nominal flyby altitude is 400 km.

primary results of these Monte Carlo simulations are the total ΔV amounts that are required to execute the targeted TCMs instead of the B-plane errors of the last flyby. The extra TCM(s) could be placed at any time between the flybys, so we picked a variety of possible manuever(s) times and ran a separate 100-run Monte Carlo simulation for each of them.

Triple-satellite-aided capture. For our nominal Callisto-Ganymede-Io-JOI (CGIJ) triple-satellite-aided capture sequence, we chose 36 different sets of maneuver times with the times of TCMs 2 and 3 independently ranging from 3.5 hours to 8.5 hours after the first and second flyby, respectively. We chose 3.5 hours as a minimum because it takes 30–50 minutes for light (e.g. radiometric information) to travel from Jupiter to Earth, some computational time to process that information into usable radiometric observables, some computational time to calculate an orbit determination solution, some computational time to target the TCM, some human decision-making time, and 30–50 minutes to upload the maneuver command to the spacecraft. Although this process could theoretically be completely automated on the ground with arbitrarily powerful computers and take less than 2 hours, we assume 3.5 hours after the flyby as a minimum to give some margin for error. (Additionally, autonomous flyby navigation could allow the TCM to be placed at any time during or after the flyby.) We use 8.5 hours as a maximum because the Io flyby is 10.5 hours after the Ganymede flyby and TCMs too close to the next flyby become inefficient.

Just like with the ballistic navigation simulations, we use both a radiometric-only navigation strategy and a combined radiometric and optical navigation strategy to simulate these flyby sequences. For radiometric navigation, the $\mathbf{B} \cdot \mathbf{T}$ error of the first flyby is 5 km and the $\mathbf{B} \cdot \mathbf{R}$ error of the first flyby is 7 km. For the second and third flybys, the $\mathbf{B} \cdot \mathbf{R}$ error becomes 5 km because the radiometric observations of the first flyby improves the out-of-plane knowledge of the spacecraft and of Jupiter. With the combined radiometric and optical navigation strategy, the B-plane error of the first flyby is 2 km in the $\mathbf{B} \cdot \mathbf{T}$ direction and 3 km in the $\mathbf{B} \cdot \mathbf{R}$ direction. These errors are slightly reduced for the second (1.5 km and 2.3 km) and third (2 km and 2.3 km) flybys. (The Io $\mathbf{B} \cdot \mathbf{R}$ error is slightly larger than the Ganymede error because Ganymede's ephemerides are better determined from optical observation than Io's, see Figure 1.) For both of the navigation strategies, TCMs 1 and 2 are used to target the Callisto and Ganymede B-planes, respectively, that minimize the Io B-plane error from its nominal value rather than targeting the nominal Callisto and Ganymede B-planes. This strategy can save a substantial amount of statistical ΔV versus sequentially targeting the nominal B-planes of all three moons. Since there are 36 Monte Carlo simulations for both radiometric-only and combined radiometric and optical, there are a total of 72 sets of 100 Monte Carlo simulations. For each set of Monte Carlo simulations, we give the median amount of statistical ΔV required to navigate the CGIJ sequence. For the radiometric-only sets, we record the median total statistical ΔV in Table 6. For the combined radiometric and optical sets, we record the median total statistical ΔV in Table 7.

We note that the median statistical ΔV results in Tables 6 and 7 indicate that only a small amount of statistical ΔV is required to navigate triple-satellite-aided capture sequences if the spacecraft is capable of implementing TCMs in between flyby. The deterministic ΔV savings in the JOI maneuvers of triple-satellite-aided capture sequences (see Table 1) more than offsets the small amount of statistical ΔV required for these TCMs.

Double-satellite-aided capture. Even though ballistic navigation methods can effectively navigate double-satellite-aided capture sequences, inserting an extra TCM in between the two flybys

Table 6. Median statistical ΔV results for radiometric-only navigation of CGIJ sequence.

	TCM 2 time[a]					
TCM 3 time[b]	3.5 hrs	4.5 hrs	5.5 hrs	6.5 hrs	7.5 hrs	8.5 hrs
3.5 hrs	3.93 m/s	4.28 m/s	4.17 m/s	4.44 m/s	5.19 m/s	5.43 m/s
4.5 hrs	3.90 m/s	4.67 m/s	4.52 m/s	5.05 m/s	5.47 m/s	5.86 m/s
5.5 hrs	4.48 m/s	4.95 m/s	4.83 m/s	5.20 m/s	5.44 m/s	6.19 m/s
6.5 hrs	5.40 m/s	5.14 m/s	5.30 m/s	5.90 m/s	5.96 m/s	6.52 m/s
7.5 hrs	5.85 m/s	6.24 m/s	6.16 m/s	6.43 m/s	6.79 m/s	7.77 m/s
8.5 hrs	7.49 m/s	7.69 m/s	8.20 m/s	8.59 m/s	8.46 m/s	8.62 m/s

[a] TCM 2 times (column headings) are in hours after closest approach to Callisto.
[b] TCM 3 times (row headings) are in hours after closest approach to Ganymede.

Table 7. Median statistical ΔV results for radiometric-only navigation of CGIJ sequence.

	TCM 2 time[a]					
TCM 3 time[b]	3.5 hrs	4.5 hrs	5.5 hrs	6.5 hrs	7.5 hrs	8.5 hrs
3.5 hrs	1.71 m/s	1.86 m/s	1.85 m/s	2.00 m/s	2.13 m/s	2.28 m/s
4.5 hrs	1.73 m/s	1.84 m/s	2.11 m/s	2.22 m/s	2.12 m/s	2.31 m/s
5.5 hrs	2.00 m/s	2.01 m/s	2.16 m/s	2.29 m/s	2.47 m/s	2.54 m/s
6.5 hrs	2.08 m/s	2.30 m/s	2.31 m/s	2.43 m/s	2.46 m/s	2.72 m/s
7.5 hrs	2.56 m/s	2.61 m/s	2.60 m/s	2.84 m/s	2.90 m/s	3.02 m/s
8.5 hrs	3.12 m/s	3.13 m/s	3.43 m/s	3.28 m/s	3.38 m/s	3.56 m/s

[a] TCM 2 times (column headings) are in hours after closest approach to Callisto.
[b] TCM 3 times (row headings) are in hours after closest approach to Ganymede.

Table 8. Median statistical ΔV results for navigation of GIJ sequence.

TCM 2, time after Ganymede flyby	3 hrs	4 hrs	5 hrs	6 hrs	7 hrs	8 hrs
Radiometric-only	2.45 m/s	2.76 m/s	3.14 m/s	3.71 m/s	4.81 m/s	6.11 m/s
Radiometric and OpNav	1.67 m/s	1.90 m/s	2.17 m/s	2.50 m/s	3.43 m/s	5.24 m/s

allows for more control over the flyby conditions of the second flyby. For the nominal Ganymede-Io-JOI sequence, the extra TCM reduces the maximum flyby B-plane error of the Io flyby from about 100 km to less than 20 km for radiometric-only navigation. The statistical ΔV cost of this extra TCM is smaller than the extra 2 TCMs in the CGIJ triple-satellite-aided capture sequence and is recorded for both the radiometric-only strategy and the combined radiometric and optical navigation strategy for several different times of TCM 2 in Table 8.

DISCUSSION

We note that this paper represents an initial attempt to solve the navigation problem for multiple-satellite-aided capture sequences. As such, these results must be analyzed within their proper context. Although the force model used to integrate these trajectories had a high degree of fidelity for a deterministic nominal trajectory, it did not incorporate unmodeled accelerations. Further, the low-order covariance analysis did not take into account the complexities of radiometric and optical navigation. For example, we ignored the large amount of data processing necessary to obtain range and range-rate observables from radiometric data. We also substantially simplified the optical navigation process by assuming angular data with a certain fixed angular covariance instead of modeling the complex image processing required to transform an OpNav picture to usable angular data. Additionally, we assumed that all of the errors in the observables and maneuver execution errors had a gaussian distribution. We also did not incorporate practical complexities such as moon visibility, star tracking, solar conjunction, Jupiter eclipsing its moons, or moons blocking radio signals.

The statistical ΔV analysis also contains a variety of simplifications. Instead of using several TCMs to correct the trajectory before the first flyby, we assume that all of the corrections are incorporated into TCM 1 a day before the first flyby. We also artificially perturb the trajectory to simulate the ephemeris errors instead of perturbing the ephemerides themselves. This artificial method of estimating the statistical ΔV decreased the fidelity of these results and did not allow the testing of several potential strategies for navigating these sequences, including using 2 TCMs before the first flyby: the first TCM to target the desired position of the second TCM.[35] Additionally, in our analysis of navigation strategies that included TCMs in between flybys, we assumed the operational capacity to perform orbit determination, target a TCM, and execute that TCM within a much shorter amount of time than the minimum amount of time used by cassini.[35]

CONCLUSIONS

Multiple-satellite-aided capture uses gravity assists of several of Jupiter's Galilean moons to capture a spacecraft into orbit around Jupiter. We motivated the navigation analysis of these trajectories by presenting the deterministic ΔV savings available for future missions to Jupiter that would use

multiple-satellite-aided capture. The main challenge in the navigation of these sequences is that small flyby errors in the first flyby of these sequences cause much larger flyby errors in subsequent flybys. Additionally, the flybys occur in rapid succession so it is operationally difficult to correct the trajectory by inserting trajectory correction maneuvers (TCMs) in between flybys.

Two direct trajectories from Earth to Jupiter capture were used as nominal trajectories for this navigational analysis: a Callisto-Ganymede-Io-JOI triple-satellite-aided capture sequence and a Ganymede-Io-JOI double-satellite-aided capture sequence. A low-order covariance analysis was performed on these nominal trajectories using simulated radiometric and optical observables to estimate the initial flyby errors. The results of this low-order covariance analysis were incorporated into Monte Carlo simulations that used a variety of navigation strategies.

With these Monte Carlo simulations, we showed that double-satellite-aided capture is likely feasible with current navigation technology using the ballistic strategy without any TCMs in between flybys. We also showed that the statistical ΔV required to precisely navigate double- or triple-satellite-aided capture sequence is low if the navigational and operational capacity to implement TCMs in between flybys is developed. Because of the deterministic ΔV savings of these multiple-satellite-aided capture sequences and their demonstrated navigational feasibility, we recommend that multiple-satellite-aided capture be strongly considered for future Jupiter missions.

ACKNOWLEDGMENTS

The authors thank Shyam Bhaskaran at the Jet Propulsion Laboratory and Geoff Wawrzyniak of Purdue University for their helpful suggestions. The first author is supported by Purdue University's Bilsland Dissertation Fellowship and Purdue Forever Fellowship.

REFERENCES

[1] R. W. Longman, "Gravity Assist from Jupiter's Moons for Jupiter-Orbiting Space Missions," tech. rep., The RAND Corp., Santa Monica, CA, 1968.

[2] R. W. Longman and A. M. Schneider, "Use of Jupiter's Moons for Gravity Assist," *Journal of Spacecraft and Rockets*, Vol. 7, No. 5, May 1970, pp. 570–576.

[3] J. K. Cline, "Satellite Aided Capture," *Celestial Mechanics*, Vol. 19, May 1979, pp. 405–415.

[4] K. T. Nock and C. Uphoff, "Satellite Aided Orbit Capture," *AAS Paper 79-165, Proceedings of the AAS/AIAA Astrodynamics Specialist Conference*, Provincetown, MA, June 25–27, 1979.

[5] M. MacDonald and C. McInnes, "Spacecraft Planetary Capture Using Gravity-Assist Maneuvers," *Journal of Guidance, Control, and Dynamics*, Vol. 28, March-April 2005, pp. 365–368.

[6] C. H. Yam, *Design of Missions to the Outer Planets and Optimization of Low-Thrust, Gravity-Assist Trajectories via Reduced Parameterization*. PhD thesis, School of Aeronautics and Astronautics, Purdue University, West Lafayette, IN, May 2008, pp. 96–104.

[7] M. Okutsu, C. H. Yam, and J. M. Longuski, "Cassini End-of-Life Escape Trajectories to the Outer Planets," *AAS Paper 07-258, Proceedings of the AAS/AIAA Astrodynamics Specialist Conference*, Mackinac Island, MI, August 2007.

[8] M. G. Wilson, C. L. Potts, R. A. Mase, C. A. Halsell, and D. V. Byrnes, "Manuever Design for Galileo Jupiter Approach and Orbital Operations," *Space Flight Dynamics, Proceedings of the 12th International Symposium*, Darmstadt, Germany, June 1997.

[9] J. R. Johannesen and L. A. D'Amario, "Europa Orbiter Mission Trajectory Design," *AAS Paper 99-330, Proceedings of the AAS/AIAA Astrodynamics Conference*, Vol. 103, Girdwood, AK, August 1999.

[10] D. Landau, N. Strange, and T. Lam, "Solar Electric Propulsion with Satellite Flyby for Jovian Capture," *Proceedings of the AAS/AIAA Spaceflight Mechanics Conference*, San Diego, CA, February 2010.

[11] A. E. Lynam, K. W. Kloster, and J. M. Longuski, "Multiple-satellite-aided Capture Trajectories at Jupiter using the Laplace Resonance," *Celestial Mechanics and Dynamical Astronomy*, Vol. 109, No. 1, 2011.

[12] J. Carrico and E. Fletcher, "Software Architecture and Use of Satellite Tool Kit's Astrogator Module for Libration Point Orbit Missions," *Libration Point Orbits and Applications: Proceedings of the Conference*, Parador d'Aiguablava, Girona, Spain, June 2002.

[13] A. E. Lynam and J. M. Longuski, "Interplanetary Trajectories for Multiple Satellite-Aided Capture at Jupiter," *AIAA Paper 2010-8254, AIAA/AAS Astrodynamics Specialists Conference*, Toronto, ON, Canada, August 2010.

[14] R. J. Haw, P. G. Antreasian, T. P. McElrath, E. J. Graat, and F. T. Nicholson, "Navigating Galileo at Jupiter Arrival," *Journal of Spacecraft and Rockets*, Vol. 34, No. 4, July-August 1997.

[15] M. Guman, D. C. Roth, and B. G. Williams, "Navigation Feasibility Studies for the Europa Orbiter Mission," *AAS Paper 98-108, Proceedings of the AAS/AIAA Space Flight Mechanics Meeting*, Monterey, CA, February 1998.

[16] B. Raofi, M. Guman, and C. Potts, "Preliminary Statistical Delta-V Analysis for a Representative Europa Orbiter Mission," *AIAA/AAS Astrodynamics Specialist Conference*, Denver, CO, August 2000.

[17] B. M. Portock, R. Haw, and L. A. D'Amario, "2003 Mars Exploration Rover Orbit Determination using Delta-VLBI Data," *AIAA Paper 02-0262, AIAA/AAS Astrodynamics Specialist Conference*, Monterey, CA, August 2002.

[18] D. Roth, P. Antreasian, J. Bordi, K. Criddle, R. Ionasescu, R. Jacobson, J. Jones, M. C. Meed, I. Roundhill, and J. Stauch, "Cassini Orbit Reconstruction from Jupiter to Saturn," *AAS Paper 05-311, Proceedings of the AAS/AIAA Astrodynamics Specialist Conference*, Lake Tahoe, CA, August 2005.

[19] K. B. Clark, T. Magner, R. Pappalardo, M. Blanc, R. Greeley, J. P. Lebreton, C. Jones, and J. C. Sommerer, "Jupiter Europa Orbiter Mission Study 2008: Final Report," tech. rep., Task Order No.: NMO710851, JPL, Pasadena, CA, 2009.

[20] J. H. Lieske, "Galilean Satellite Ephemerides E5," *Astronomy and Astrophysics Supplement*, Vol. 129, 1998.

[21] R. A. Jacobson, "Jup230 - JPL satellite ephemeris," ssd.jpl.nasa.gov/?sat_ephem, 2003.

[22] D. L. Jones, E. Fomalont, V. Dhawan, J. Romney, W. M. Folkner, G. Lanyi, J. Border, and R. A. Jacobson, "Very Long Baseline Array Astrometric Observations of the Cassini Spacecraft at Saturn," *The Astronomical Journal*, Vol. 141, 2011.

[23] W. M. Owen, "Methods of Optical Navigation," *AAS Paper 11-215, Proceedings of the AAS/AIAA Space Flight Mechanics Meeting*, New Orleans, LA, February 2011.

[24] S. Bhaskaran, S. D. Desai, D. P. J., B. M. Kennedy, G. W. Null, W. M. Owen Jr., J. E. Riedel, S. P. Synnott, and R. A. Werner, "Orbit Determination Performance Evaluation of the Deep Space 1 Autonomous Navigation System," *Proceedings of the AAS/AIAA Space Flight Mechanics Meeting*, Monterey, CA, Feb. 1998.

[25] S. Bhaskaran, J. E. Riedel, S. P. Synnott, and T. C. Wang, "The Deep Space 1 Autonomous Navigation System: A Post-Flight Analysis," *Paper AIAA 2000-3935, AIAA/AAS Astrodynamics Specialist Conference*, Denver, CO, Aug. 2000.

[26] D. G. Kubitschek, N. Mastrodemos, R. A. Werner, B. M. Kennedy, S. P. Synnott, G. W. Null, S. Bhaskaran, J. E. Riedel, and A. T. Vaughan, "Deep Impact Autonomous Navigation: The Trials of Targeting the Unknown," *AAS Paper 06-081, Proceedings of the AAS Guidance and Control Conference*, Breckenridge, CO, Feb. 2006.

[27] D. G. Kubitschek, N. Mastrodemos, R. A. Werner, S. P. Synnott, S. Bhaskaran, J. E. Riedel, B. M. Kennedy, G. W. Null, and A. T. Vaughan, "The Challenges of Deep Impact Autonomous Navigation," *Journal of Field Robotics*, Vol. 24, No. 4, April 2007.

[28] Y. Cheng and J. K. Miller, "Autonomous Landmark Based Spacecraft Navigation System," *AAS Paper 03-223, Proceedings of the AAS/AIAA Spaceflight Mechanics Meeting*, Ponce, Puerto Rico, Feb. 2003.

[29] T. J. Martin-Mur, S. Bhaskaran, R. J. Cesarone, and T. McElrath, "The Next 25 Years of Deep Space Navigation," *AAS Paper 08-057, Proceedings of the AAS Guidance and Control Conference*, Breckenridge, CO, Feb. 2008.

[30] J. E. Riedel, S. Bhaskaran, D. B. Eldred, R. A. Gaskell, C. A. Grasso, B. M. Kennedy, D. G. Kubitschek, N. Mastrodemos, S. P. Synnott, A. T. Vaughan, and R. A. Werner, "AutoNav Mark3: Engineering the Next Generation of Autonomous Onboard Navigation and Guidance," *AAS Paper 08-057, Proceedings of the AAS Guidance and Control Conference*, Breckenridge, CO, Feb. 2008.

[31] T. D. Goodson, D. L. Gray, Y. Hahn, and F. Peralta, "Cassini Maneuver Experience: Finishing Inner Cruise," *AAS Paper 00-167, Proceedings of the AAS/AIAA Spaceflight Mechanics Meeting*, Clearwater, FL, January 2000.

[32] S. V. Wagner and T. D. Goodson, "Execution-Error Modeling and Analysis of the Cassini-Huygens Spacecraft through 2007," *AAS Paper 08-113, Proceedings of the AAS/AIAA Space Flight Mechanics Meeting*, Galveston, TX, January 2008.

[33] E. M. Gist, C. G. Ballard, Y. Hahn, P. W. Stumpf, S. V. Wagner, and P. N. Williams, "Cassini Maneuver Experience: First Year of the Equinox Mission," *AAS Paper 09-349, Proceedings of the AAS/AIAA Astrodynamics Specialists Conference*, Pittsburgh, PA, August 2009.
[34] C. R. Gates, "A Simplified Model of Midcourse Maneuver Execution Errors," tech. rep., Jet Propulsion Laboratory, Pasadena, CA, 1963.
[35] C. G. Ballard, J. Arrieta, Y. Hahn, P. W. Stumpf, S. V. Wagner, and P. N. Williams, "Cassini Maneuver Experience: Ending the Equinox Mission," *AIAA Paper 2010-8257, AIAA/AAS Astrodynamics Specialists Conference*, Toronto, ON, CA, August 2010.

APPENDIX: DEFINING B-PLANE PARAMETERS

We use a B-plane parameters to characterize the flyby errors in these sequences rather than simply flyby altitudes in order to take out-of-plane errors into account. The spacecraft has two B-plane parameters that are used to characterize each flyby: $\mathbf{B} \cdot \mathbf{T}$ and $\mathbf{B} \cdot \mathbf{R}$. (This description of the B-plane is similar to that given by Macdonald and McInnes.[5]) In Fig. 5, the B-plane parameters are defined. The $\mathbf{S}$ vector is defined as a unit vector parallel to the spacecraft's incoming hyperbolic asymptote (with respect to the moon, not Jupiter). The $\mathbf{T}$ vector is defined as the normalized cross product of the $\mathbf{S}$ vector and the moon's orbit normal, $\mathbf{N}$:

$$\mathbf{T} = \frac{\mathbf{S} \times \mathbf{N}}{|\mathbf{S} \times \mathbf{N}|} \tag{1}$$

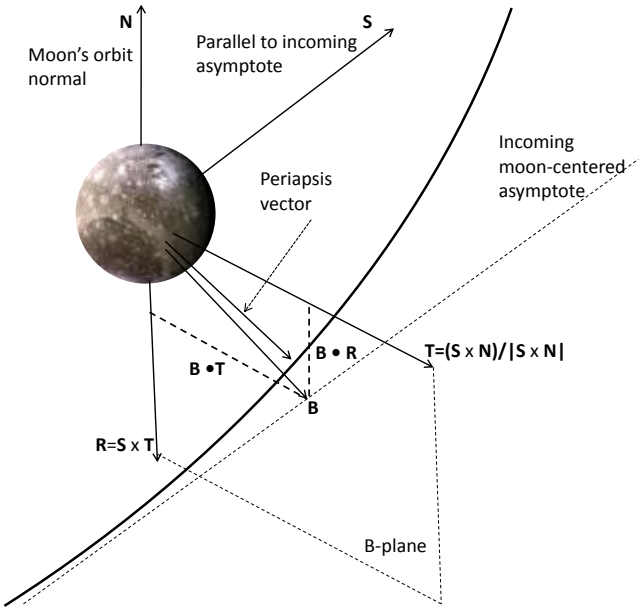

Figure 5. A graphical depiction of the B-plane used to describe the spacecraft's flyby of a Galilean moon.

As illustrated in Fig. 5, the $\mathbf{R}$ vector is orthogonal to $\mathbf{T}$ and $\mathbf{S}$ such that

$$\mathbf{R} = \mathbf{S} \times \mathbf{T} \tag{2}$$

The B-plane is a plane defined by the $\mathbf{R}$ and $\mathbf{T}$ vectors and centered at the moon's center of mass. The B-plane is, by definition, perpendicular to the incoming moon-centered asymptote. The $\mathbf{B}$ vector is the distance from the center of mass of the moon to the incoming moon-centered asymptote's

intersection with the B-plane (as shown in Fig. 5). The B-plane parameters, $\mathbf{B} \cdot \mathbf{T}$ and $\mathbf{B} \cdot \mathbf{R}$, are the two components of the $\mathbf{B}$ vector in the $\mathbf{T}$ and $\mathbf{R}$ directions, respectively.

Since all of these multiple-satellite-aided capture trajectories are nearly within Jupiter's equatorial plane, $\mathbf{S}$ is nearly perpendicular to $\mathbf{N}$ such that $\mathbf{N}$ and $\mathbf{R}$ are nearly anti-parallel. Under the anti-parallel assumption, $\mathbf{B} \cdot \mathbf{T}$ is defined as the equatorial component of $\mathbf{B}$ and $\mathbf{B} \cdot \mathbf{R}$ as the polar or out-of-plane component of $\mathbf{B}$. Hence, a flyby with a $\mathbf{B} \cdot \mathbf{T}$ component of zero and a large $\mathbf{B} \cdot \mathbf{R}$ component would be a polar flyby. Similarly, a flyby with a large $\mathbf{B} \cdot \mathbf{T}$ component and a $\mathbf{B} \cdot \mathbf{R}$ component of zero would be an equatorial flyby. Jupiter's Galilean moons are all tidally locked, so their orbit planes are parallel to their equatorial planes. Within the Monte Carlo simulations, the gaussian B-plane targeting errors are estimated for each navigation strategy by using the position covariance of the spacecraft relative to the Galilean moons.